A PRIMAL-DUAL APPROACH FOR DISCONTINUITY PRESERVING REGISTRATION

Silja Kiriyanthan *Ketut Fundana* *Tahir Majeed* *Philippe C. Cattin*

Medical Image Analysis Center
University of Basel
Switzerland

ABSTRACT

Image registration is a powerful tool in medical image analysis and facilitates the clinical routine in several aspects. There are many well established non-rigid registration methods, but those which are able to preserve discontinuities in the displacement field are rather rare. This paper deals with a non-rigid registration method, that can handle discontinuities in the motion field that appear in particular at organ boundaries during the breathing induced organ motion. Due to the fact that motion segmentation could play a guiding role during discontinuity preserving registration, we therefore embed the registration method in a segmentation framework. Furthermore, we are able to use a primal-dual method to estimate a solution to this complex variational problem. Experimental results are presented for MR Images with apparent breathing induced sliding motion of the liver along the abdominal wall.

***Index Terms*—** Motion segmentation, registration, discontinuity preserving, primal-dual approach

1. INTRODUCTION

Image registration became an indispensable tool for many medical applications including Image-Guided Therapy systems. Today's image registration methods are powerful at handling rigid as well as non-rigid motion on mono- and multi-modal images. With the introduction of imaging technologies capable of capturing 4D organ motion, such as 4D-MRI, 4D-CT or 4D-Ultrasound, imagery of sliding organs became a significant focus of research [1, 2]. Most of the state-of-the-art image registration methods cannot yet properly deal with these data sets, as their regularisations force continuous motion fields over the organ boundaries.

In recent publications, the concept of direction-dependent regularisation of the displacement field, has been introduced to preserve discontinuities in the motion field, *e.g.* [2]. The drawback of these methods is the necessity of providing a good manual segmentation of the organ boundaries.

In 1989, Mumford and Shah proposed in their pioneering work [3] a functional that avoids spatial smoothing in certain locations of the image, thus preserving discontinuities. Vese and Chan [4] then introduced a level set framework based approach to efficiently solve the Mumford and Shah minimisation problem for segmentation. Another influential approach, known to preserve discontinuities and proposed by Rudin, Osher and Fatemi [5] (the ROF-model), is based on the Total Variation (TV) norm. The beneficial behaviour of the TV-norm was also exploited in recent registration and optical flow methods, as for example by [6, 7].

As motion discontinuities mainly appear at object boundaries, it seems natural to combine motion segmentation and registration. Given a good motion segmentation, a proper discontinuous motion field can be estimated and vice versa. Recent research [8] tried to leverage this property by combining motion segmentation with registration.

Here we deal with a non-rigid registration method that is able to handle discontinuities in the motion field by combining motion segmentation and registration. For the motion segmentation we make use of Chan *et al.*'s framework [9] that guarantees a globally optimal solution for a fixed motion field. In contrast to our previous work [10], where we used an approximation for the TV-norm, this time the proposed energy functional is regularised with the pure TV-L^1 for both, the motion segmentation and the displacement field. Solving TV-L^1 based functionals is, however, inherently difficult and in this paper we show how to solve the proposed energy functional by exploiting the primal-dual method of Chambolle and Pock [7], which is very efficient for a wide class of non-smooth problems.

2. REGISTRATION AND MOTION SEGMENTATION

Let $\Omega \subset \mathbb{R}^2$ be the domain of the pixel positions $\vec{x} = (x_1, x_2)$. We then define by the functions $R : \Omega \to \mathbb{R}$ and $T : \Omega \to \mathbb{R}$ our reference and template image. The aim of image registration is to find a transformation $\Phi(\vec{x}) := \vec{x} + \vec{w}(\vec{x})$ such that the relation $T \circ \Phi \approx R$ holds. The function $\vec{w}(\vec{x}) := (u(\vec{x}), v(\vec{x}))$, with $u, v : \Omega \to \mathbb{R}$, describes the displacement field and will be the intrinsic function we investigate. For convenience we will use the abbreviations $\vec{w}$, u and v for $\vec{w}(\vec{x})$, $u(\vec{x})$ and $v(\vec{x})$.

To solve a non-rigid registration problem with expected discontinuities in the displacement field, we want to follow a variational approach and we therefore need to define an en-

This work has been funded by Dr. Hansjörg Wyss.

ergy functional. To integrate the formulation of the energy functional into the convex segmentation model of Chan *et al.* [9] to differentiate the displacement field $\vec{w}$ into $\vec{w}^+$ and $\vec{w}^-$, we introduce the binary function $\tilde{u}(\vec{x}) := \mathbf{1}_\Sigma(\vec{x})$, where $\Sigma \subseteq \Omega \subseteq \mathbb{R}^2$, with $\Sigma := \{\vec{x} \in \Omega \,|\, \tilde{u}(\vec{x}) = 1\}$. By defining $D(\vec{w}) := f(\vec{w}) + \mu\, s(\vec{w})$ as a data term, with

$$\begin{aligned} f(\vec{w}) = f(u,v) := \gamma_1 |T(\vec{x}+\vec{w}) - R(\vec{x})| \\ + \gamma_2 |\partial_{x_1} T(\vec{x}+\vec{w}) - \partial_{x_1} R(\vec{x})| \\ + \gamma_2 |\partial_{x_2} T(\vec{x}+\vec{w}) - \partial_{x_2} R(\vec{x})|\,, \end{aligned} \quad (1)$$

and

$$s(\vec{w}) = s(u,v) := \sqrt{|\nabla u|^2 + |\nabla v|^2} = |\nabla \vec{w}|\,, \quad (2)$$

the fidelity respectively the smoothness term and $\gamma_1, \gamma_2 \in \mathbb{R}_0^+$, $\mu \in \mathbb{R}^+$ weighting parameters, we formulate our energy functional as

$$\begin{aligned} E(\vec{w}^+, \vec{w}^-, \tilde{u}) = \int_\Omega D(\vec{w}^+)\, \tilde{u}(\vec{x})\, d\vec{x} + \int_\Omega D(\vec{w}^-)\, (1 - \tilde{u}(\vec{x}))\, d\vec{x} \\ + \int_\Omega |\nabla \tilde{u}(\vec{x})|\, d\vec{x}\,, \end{aligned} \quad (3)$$

where the last term of the above energy is a regularisation defined by the TV norm.

Remark. As pointed out by Chan *et al.* in [9], (3) is strongly related to the Mumford-Shah functional [3] and one can show, that a global minimiser Σ_{min} can be found by solving the convexified problem $\min_{0 \le \tilde{u} \le 1} E(\vec{w}^+, \vec{w}^-, \tilde{u})$ and finally setting $\Sigma = \Sigma(\eta) := \{\vec{x} \in \Omega \,|\, \tilde{u}(\vec{x}) \ge \eta\}$ for almost every η with $\eta \in [0,1]$. In fact, this holds for any data terms $D(\vec{w}^+)$ and $D(\vec{w}^-)$ that are measurable.

Finally, we obtain the aimed displacement field by setting $\vec{w} := \vec{w}^+\, \tilde{u} + \vec{w}^-\, (1 - \tilde{u})$.

3. MINIMISATION

3.1. Iterative Scheme

To facilitate the minimisation procedure we approximate the fidelity term f in (1) by first order Taylor expansions and get

$$f(\vec{w}) = \gamma_1 |\rho_1(\vec{w})| + \gamma_2 |\rho_2^{(1)}(\vec{w})| + \gamma_2 |\rho_2^{(2)}(\vec{w})|\,, \quad (4)$$

where

$$\rho_1(\vec{w}) := T(\vec{x}+\vec{w}_0) + \nabla T(\vec{x}+\vec{w}_0)^{\mathrm{T}} (\vec{w} - \vec{w}_0) - R(\vec{x})\,, \quad (5)$$

$$\begin{aligned} \rho_2^{(1)}(\vec{w}) := \partial_{x_1} T(\vec{x}+\vec{w}_0) \\ + \begin{pmatrix} \partial_{x_1 x_1} T(\vec{x}+\vec{w}_0) \\ \partial_{x_2 x_1} T(\vec{x}+\vec{w}_0) \end{pmatrix}^{\mathrm{T}} (\vec{w} - \vec{w}_0) - \partial_{x_1} R(\vec{x})\,, \end{aligned} \quad (6)$$

and

$$\begin{aligned} \rho_2^{(2)}(\vec{w}) := \partial_{x_2} T(\vec{x}+\vec{w}_0) \\ + \begin{pmatrix} \partial_{x_1 x_2} T(\vec{x}+\vec{w}_0) \\ \partial_{x_2 x_2} T(\vec{x}+\vec{w}_0) \end{pmatrix}^{\mathrm{T}} (\vec{w} - \vec{w}_0) - \partial_{x_2} R(\vec{x})\,. \end{aligned} \quad (7)$$

The minimisation of the energy functional E with respect to $\vec{w}^+$, $\vec{w}^-$ and $\tilde{u}$ is then performed by the following iterative scheme:

1. For fixed $\vec{w}^+$ and $\vec{w}^-$, solve

$$\begin{aligned} \min_{\tilde{u} \in [0,1]} \left\{ \int_\Omega D(\vec{w}^+)\, \tilde{u}(\vec{x})\, d\vec{x} + \int_\Omega D(\vec{w}^-)\, (1 - \tilde{u}(\vec{x}))\, d\vec{x} \right. \\ \left. + \int_\Omega |\nabla \tilde{u}(\vec{x})|\, d\vec{x} \right\}. \end{aligned} \quad (8)$$

2. For fixed $\vec{w}^-$ and $\tilde{u}$, solve

$$\min_{\vec{w}^+} \left\{ \int_\Omega D(\vec{w}^+)\, \tilde{u}(\vec{x})\, d\vec{x} \right\}. \quad (9)$$

3. For fixed $\vec{w}^+$ and $\tilde{u}$, solve

$$\min_{\vec{w}^-} \left\{ \int_\Omega D(\vec{w}^-)\, (1 - \tilde{u}(\vec{x}))\, d\vec{x} \right\}. \quad (10)$$

To minimise our energy functional in (3) with respect to $\vec{w}^+$, $\vec{w}^-$ and $\tilde{u}$ in an efficient way, we follow a primal-dual approach as described by Chambolle and Pock in [7]. We therefore recapitulate in the next section the basic notations and formulations.

3.2. The Primal-Dual Approach

First, we define by X and Y two finite-dimensional real vector spaces. Their inner products are denoted by $\langle \cdot, \cdot \rangle_X$ respectively $\langle \cdot, \cdot \rangle_Y$ and their induced norms are given by $\|\cdot\|_X = \sqrt{\langle \cdot, \cdot \rangle_X}$ respectively $\|\cdot\|_Y = \sqrt{\langle \cdot, \cdot \rangle_Y}$. The general nonlinear primal problem we consider is of the form

$$\min_{x \in X} F(Kx) + G(x)\,, \quad (11)$$

where $F : Y \to [0, +\infty)$ and $G : X \to [0, +\infty)$ are proper, convex and lower semi-continuous and the map $K : X \to Y$ is a continuous linear operator. The corresponding primal-dual formulation of (11) is the saddle-point problem

$$\min_{x \in X} \max_{y \in Y} \langle Kx, y \rangle_Y + G(x) - F^*(y)\,, \quad (12)$$

with $F^* : Y \to \mathbb{R} \cup \{+\infty\}$ being the convex conjugate of F. It is assumed that the problems above have at least one solution $(\hat{x}, \hat{y}) \in X \times Y$ and therefore it holds $K\hat{x} \in \partial F^*(\hat{y})$ and $-(K\hat{y}) \in \partial G(\hat{x})$, where $\partial F^*(\hat{y})$ and $G(\hat{x})$ are the subdifferentials of the convex functions F^* at $\hat{y}$ and G at $\hat{x}$. Furthermore it is assumed that F and G are "simple", i.e. that the resolvent operators $(I + \sigma \partial F^*)^{-1}$ and $(I + \tau \partial G)^{-1}$ are easy to compute, as they are needed later in the approach. For a convex function f the resolvent of the operator $\tau \partial f$ at $\tilde{x}$ can be calculated in our case by

$$x = (I + \tau \partial f)^{-1}(\tilde{x}) = \arg\min_x \left\{ \frac{\|x - \tilde{x}\|^2}{2\tau} + f(x) \right\}. \quad (13)$$

In this paper we will only make use of Algorithm 1 in [7] with the extrapolation parameter $\theta = 1$. Although interesting, the usage of the other proposed algorithms is left for the moment for later research.

To apply Algorithm 1 in [7] to the minimisation problems (8), (9) and (10), we first need to rewrite them in their discretised version, then identify the functions F and G and finally derive the resolvent operators $(I + \sigma \partial F^*)^{-1}$ and $(I + \tau \partial G)^{-1}$. For the discrete setting we therefore define by $\vec{x}_{i,j} = (x_{1\,i,j}, x_{2\,i,j}) = (ih, jh)$, $i = 1, \ldots, M$, $j = 1, \ldots, N$, the pixel positions in the image domain with h

being the spatial step size. For further details we refer the reader to [7] and the references therein.

In the following sections we will derive the resolvent operators for the three minimisation problems (8), (9) and (10).

3.3. Resolvent Operators for Problem (8)

To discretise the continuous problem (8) we will make use of the spaces $X = \mathbb{R}^{MN}$ and $Y = X \times X$ and their corresponding inner products. Using the rectangle rule we can rewrite problem (8) in the discretised version

$$h^2 \min_{\tilde{u}\in[0,1]^{MN}} \left\{ \|\nabla \tilde{u}\|_1 + \sum_{i,j} \Big(D(\vec{w}^+_{i,j})\tilde{u}_{i,j} + D(\vec{w}^-_{i,j})(1-\tilde{u}_{i,j}) \Big) \right\}, \quad (14)$$

where the factor h^2 can be neglected, since it has no influence on the optimal solution. The norm $\|\nabla s\|_1$, with $s \in X$, is defined by $\|\nabla s\|_1 = \sum_{i,j} |(\nabla s)_{i,j}|$, where $|(\nabla s)_{i,j}| = \sqrt{\left((\nabla s)^{(1)}_{i,j}\right)^2 + \left((\nabla s)^{(2)}_{i,j}\right)^2}$.

Comparing (14) to (11), we see that $K = \nabla$, $F(\nabla \tilde{u}) = \|\nabla \tilde{u}\|_1$ and $G(\tilde{u}) = \sum_{i,j} D(\vec{w}^+_{i,j})\,\tilde{u}_{i,j} + D(\vec{w}^-_{i,j})\,(1-\tilde{u}_{i,j})$. The solution of the resolvent operator with respect to F^* is

$$p = (I + \sigma \partial F^*)^{-1}(\tilde{p}) \Longrightarrow p_{i,j} = \frac{\tilde{p}_{i,j}}{\max\{1, |\tilde{p}_{i,j}|\}},$$

and the one with respect to G

$$\tilde{u} = (I + \tau \partial G)^{-1}(\hat{u}) \Longrightarrow$$
$$\tilde{u}_{i,j} = \min\left\{ \max\left\{ \hat{u}_{i,j} - \tau \left(D(\vec{w}^+_{i,j}) - D(\vec{w}^-_{i,j}) \right), 0 \right\}, 1 \right\}.$$

3.4. Resolvent Operators for Problem (9)

If we have a closer look at the continuous minimisation problem (9), we see that we only receive information about $\vec{w}^+$ on the domain Σ where $\tilde{u}$ will be set to 1. Although theoretically reasonable, for the numerical calculations the implementation gets facilitated by having a smooth extension of $\vec{w}^+$ to the domain $\Omega \setminus \Sigma$. We therefore consider instead

$$\min_{\vec{w}^+} \left\{ \int_\Omega f(\vec{w}^+)\,\tilde{u}(\vec{x}) + \mu\, s(\vec{w}^+)\, d\vec{x} \right\}. \quad (15)$$

Comparing (9) to (15) the only difference is, that the factor $\tilde{u}$ is not applied to the smoothness term s anymore. For the primal-dual approach we will use this time the spaces $X = \mathbb{R}^{MN} \times \mathbb{R}^{MN}$ and $Y = X \times X$ and their corresponding inner products. After the discretisation of problem (15) we obtain

$$\min_{\vec{w}^+ \in X} \Big\{ \mu \|\nabla \vec{w}^+\|_1 + \sum_{i,j} \Big(\gamma_1 |\rho_1(\vec{w}^+_{i,j})| + \gamma_2 |\rho_2^{(1)}(\vec{w}^+_{i,j})| + \gamma_2 |\rho_2^{(2)}(\vec{w}^+_{i,j})| \Big) \tilde{u}_{i,j} \Big\}, \quad (16)$$

where this time $\|\nabla s\|_1$, with $s = (s_1, s_2) \in X$, is defined by $\|\nabla s\|_1 = \sum_{i,j} |(\nabla s)_{i,j}|$ with $|(\nabla s)_{i,j}| = \sqrt{\left((\nabla s_1)^{(1)}_{i,j}\right)^2 + \left((\nabla s_1)^{(2)}_{i,j}\right)^2 + \left((\nabla s_2)^{(1)}_{i,j}\right)^2 + \left((\nabla s_2)^{(2)}_{i,j}\right)^2}$.

Comparing (16) to (11), we see that
$K = \nabla$, $F(\nabla \vec{w}^+) = \mu \|\nabla \vec{w}^+\|_1$ and $G(\vec{w}^+) = \sum_{i,j} \left(\gamma_1 |\rho_1(\vec{w}^+_{i,j})| + \gamma_2 |\rho_2^{(1)}(\vec{w}^+_{i,j})| + \gamma_2 |\rho_2^{(2)}(\vec{w}^+_{i,j})| \right) \tilde{u}_{i,j}$.

From the resolvent operator with respect to F^* we obtain

$$q = (I + \sigma \partial F^*)^{-1}(\tilde{q}) \Longrightarrow q_{i,j} = \mu \frac{\tilde{q}_{i,j}}{\max\{\mu, |\tilde{q}_{i,j}|\}}. \quad (17)$$

The derivation of the resolvent operator with respect to G is not that straightforward and more effort has to be put in to find a suitable solution. Having a closer look at the definition of G and (13), we see that we have to distinguish the cases

$$\rho_1(\vec{w}^+_{i,j}) \begin{pmatrix} > \\ < \\ = \end{pmatrix} 0\,, \rho_2^{(1)}(\vec{w}^+_{i,j}) \begin{pmatrix} > \\ < \\ = \end{pmatrix} 0\,, \rho_2^{(2)}(\vec{w}^+_{i,j}) \begin{pmatrix} > \\ < \\ = \end{pmatrix} 0\,, \quad (18)$$

which turn out to be 27 in total.

3.5. Resolvent Operators for Problem (10)

This section is very similar to Section 3.4 and we mainly have to just replace $\vec{w}^+$ by $\vec{w}^-$ and $\tilde{u}$ by $1-\tilde{u}$. To achieve a smooth extension of $\vec{w}^-$ to the domain Σ, we consider now instead of problem (10) the following problem

$$\min_{\vec{w}^-} \left\{ \int_\Omega f(\vec{w}^-)\,(1 - \tilde{u}(\vec{x})) + \mu\, s(\vec{w}^-)\, d\vec{x} \right\}. \quad (19)$$

The spaces X and Y and their inner products are defined in the same way as in Section 3.4 and the discretisation of (19) is performed in the same manner as before. The convex conjugate F^* of the resulting function F is identical to the one in the Section 3.4 and hence the corresponding resolvent operator identical to (17). Finally, compared to the section before, there are only very slight changes of the resolvent operator with respect to G.

4. RESULTS

Although, we have a convex minimisation problem with respect to the motion segmentation function $\tilde{u}$ and linearised the fidelity term f in (4) to facilitate the minimisation procedure, the overall problem remains non-convex and we have to update $\vec{w}^+_0$ and $\vec{w}^-_0$ regularly. A coarse-to-fine strategy, with minimal image size 32×32 and scaling factor 0.9, is applied to avoid the risk of getting stuck in a local minimum during the optimisation and the displacement fields $\vec{w}^+$ and $\vec{w}^-$ are initialised with $\vec{0}$. Because of the Remark in Section 2, whatever initialisation we choose for $\tilde{u}$, the global minimiser will be the same for fixed $\vec{w}^+$ and $\vec{w}^-$. By choosing a random initialisation for $\tilde{u}$, the experiments were indeed satisfying, although the displacement fields were updated regularly. The final iteration scheme consist of two loops. The outer loop iterates over the pyramid levels. In each level an inner loop updates the values for $\tilde{u}$, $\vec{w}^+$ and $\vec{w}^-$, following steps *1 - 3* in Section 3.1. Thus, in each iteration of this inner loop one step of the primal-dual Algorithm 1 from [7] is performed with the appropriate resolvent operators from the previous sections to update $\tilde{u}$, $\vec{w}^+$ and $\vec{w}^-$. Bicubic interpolation is used to calculate the images $T(\vec{x} + \vec{w}^\pm)$ during the iterations and to obtain the final registered image $T(\vec{x} + \vec{w})$.

We compare our method to other discontinuity preserving registration methods, in this case, the demon algorithm with anisotropic diffusion filtering [11] and the registration algorithm of Brox *et al.* [6].

We show the qualitative comparison of the three different methods in Fig. 1. As clearly seen, our method can achieve more crisp discontinuities in the displacement field compared to the demon algorithm with anisotropic diffusion filtering and the registration algorithm of Brox *et al.*

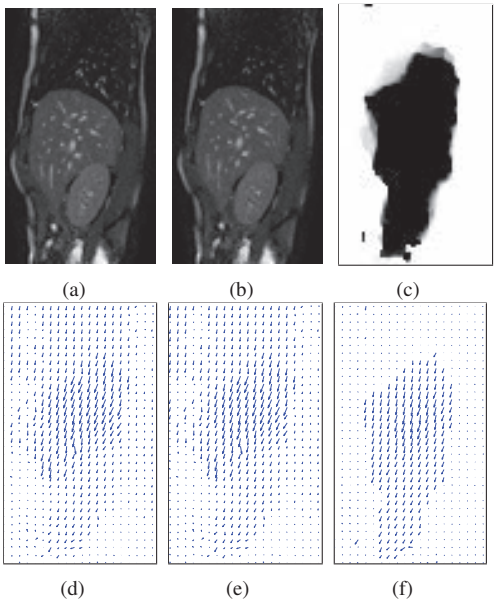


Fig. 1. The reference (a) and template (b) images, and the motion segmentation result (c). The displacement field for the demon algorithm with anisotropic diffusion filtering is shown in (d), the one for the registration algorithm of Brox *et al.* in (e) and finally the one of our method in (f).

In Fig. 2 a quantitative evaluation is shown for 22 different liver image pairs. We chose the parameters for all the three methods by optimising them with respect to these image pairs. The parameters of our method were set to $\gamma_1 = 40$, $\gamma_2 = 10$ and $\mu = 2$. For the demon algorithm with anisotropic diffusion filtering we could use the suggested parameters and for Brox *et al.*'s method we used $\gamma = 5$, $\alpha = 80$ and $\sigma = 0.9$. To asses the performance of the three methods, we calculated the mean squared error (MSE) and the normalised mutual information (NMI), with the grey values scaled from 0 to 1. For all our examples the proposed method performed better than the demon method with anisotropic diffusion and the registration algorithm of Brox *et al.* We used the Kolmogorov-Smirnov test to check for normality of the results using the R Software package (Version 2.10.1) with a significance level of 5%. The t-test showed that the proposed method performs significantly better with both $p < 0.05$.

5. CONCLUSION

In this paper we showed that the primal-dual method [7] can be used for discontinuity preserving non-rigid registration, which makes use of Chan *et al.*'s framework [9]. The so gained motion segmentation influences the motion estimation positively by sharpening the discontinuities in the displacement field. The minimisation of the energy functional is implemented in a coarse-to-fine strategy and experimental

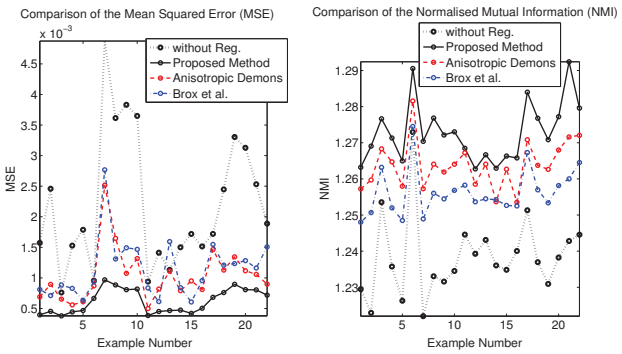


Fig. 2. Quantitative evaluation for 22 pairs of liver images with a discontinuous displacement field. Comparison of the MSE *(left)* and NMI *(right)*.

results demonstrated desirable performance of the proposed method in comparison with those of the demon algorithm with anisotropic diffusion filtering [11] and the registration algorithm of Brox *et al.* [6]. In future work we plan on including known corresponding landmarks into the functional as hard constraints.

6. REFERENCES

[1] D. Ruan, S. Esedoglu, and J. A. Fessler, "Discriminative Sliding Preserving Regularization in Medical Image Registration," in *IEEE International Symposium on Biomedical Imaging 2009*, 2009, pp. 430–433.

[2] A. Schmidt-Richberg, J. Ehrhardt, R. Werner, and H. Handels, "Slipping Objects in Image Registration: Improved Motion Field Estimation with Direction-Dependent Regularization," in *MICCAI*, 2009, vol. 5761, pp. 755–762.

[3] D. Mumford and J. Shah, "Optimal Approximations by Piecewise Smooth Functions and Associated Variational-Problems," *Communications on Pure and Applied Mathematics*, vol. 42, no. 5, pp. 577–685, Jul 1989.

[4] L. A. Vese and T. F. Chan, "A Multiphase Level Set Framework for Image Segmentation Using the Mumford and Shah Model," *IJCV*, vol. 50, no. 3, pp. 271–293, Dec 2002.

[5] L. I. Rudin, S. Osher, and E. Fatemi, "Nonlinear Total Variation Based Noise Removal Algorithms," *Physica D*, vol. 60, no. 1-4, pp. 259–268, Nov 1 1992.

[6] T. Brox, A. Bruhn, N. Papenberg, and J. Weickert, "High Accuracy Optical Flow Estimation Based on a Theory for Warping," in *Computer Vision - ECCV. Proceedings (LNCS Vol. 3024)*, 2004, pp. 25–36.

[7] A. Chambolle and T. Pock, "A First-Order Primal-Dual Algorithm for Convex Problems with Applications to Imaging," *Journal of Mathematical Imaging and Vision*, vol. 40, no. 1, pp. 120–145, Mar 2011.

[8] T. Amiaz and N. Kiryati, "Piecewise-Smooth Dense Optical Flow via Level Sets," *IJCV*, vol. 68, no. 2, pp. 111–124, Jun 2006.

[9] T. F. Chan, S. Esedoglu, and M. Nikolova, "Algorithms for Finding Global Minimizers of Image Segmentation and Denoising Models," *Siam Journal on Applied Mathematics*, vol. 66, no. 5, pp. 1632–1648, 2006.

[10] S. Kiriyanthan, K. Fundana, and Ph. C. Cattin, "Discontinuity Preserving Registration of Abdominal MR Images with Apparent Sliding Organ Motion," in *Workshop on Computational and Clinical Applications in Abdominal Imaging, MICCAI 2011, LNCS*, H. Yoshida, G. Sakas, and M. G. Linguraru, Eds., 2011, vol. 7029.

[11] D. Demirovic, A. Serifovic, and Ph. C. Cattin, "An Anisotropic Diffusion Regularized Demons for Improved Registration of Sliding Organs," in *18th International Electrotechnical and Computer Science Conference (ERK)*, 2009.